Published in Journal of Hydrology 352, issues 1-2, 16-29, 2008
which should be used for any reference to this work

A quantitative approach to spring hydrograph decomposition

Attila Kovács [a,*], Pierre Perrochet [b,1]

[a] *geokovacs.com, 15 Gyorgyhegy utca, 2083 Solymar, Hungary*
[b] *CHYN, University of Neuchâtel, Rue Emile-Argand 11, CH-2007 Neuchâtel, Switzerland*

Summary A combined analytical—numerical study for the characterization of spring hydrographs is presented. Two-dimensional analytical solutions for diffusive flux from rectangular blocks of arbitrary shape facilitate a quantitative characterization of exponential hydrograph components. Together with analytical solutions for block discharge, a systematic analysis of numerically simulated spring hydrographs of synthetic karst systems provides an insight into karst hydrodynamics.

Different hydrograph components do not represent different classes of rock permeability. Hydrographs of individual homogeneous blocks can be decomposed into several exponential components. Discharge hydrographs of symmetric rectangular blocks can be reconstructed by the sum of only three exponential components. Increasing block asymmetry results in an increasing number of exponential components contributing significantly to total discharge.

Spring hydrographs represent a sum of individual block discharges originating from diffuse infiltration and conduit discharge originating from concentrated recharge. Beyond the inflection of the recession limb, a spring hydrograph can be decomposed in a similar manner to that of individual homogeneous blocks. The presented hydrograph analytical method facilitates the estimation of hydraulic and geometric parameters of karst hydrogeological systems.

Keywords: Karst springs; Spring hydrographs; Hydrograph decomposition; Recession coefficient

Introduction

Karst aquifers differ from other types of hydrogeological systems in their complex behavior originating from strong heterogeneity. Heterogeneity manifests in the duality (diffuse and concentrated nature) of each hydraulic process taking place in karst aquifers (Király, 1994). These hydraulic

* Corresponding author. Tel./fax: +36 1 3872793.
E-mail addresses: attila.kovacs@unine.ch (A. Kovács), Pierre.Perrochate@unine.ch (P. Perrochet).
[1] Tel.: +41 32 718 2577; fax: +41 32 718 2603.

processes include infiltration, groundwater flow and discharge.

The quantitative characterization of the hydrodynamic functioning of karst systems requires the definition of realistic hydraulic and geometric parameters (Király and Morel, 1976a; Király, 1998a, 2002). Information on these parameters is far more difficult to obtain to karst systems than other kinds of hydrogeological systems. Classical geological and hydrogeological surveys, borehole tests, tracing experiments, speleological and geophysical observations provide only a limited information on the spatial configuration and hydraulic properties of a conduit network. However, in most cases spring discharge time series data, coupled with information on the hydraulic properties of the low-permeability rock matrix are available, or possible to obtain. Hydrograph analytical techniques have the potential of estimating effective hydraulic parameters and geometric characteristics of karst systems using this information.

Some hydrograph analytical techniques are based on the analysis of slow hydrograph recession segments (Maillet, 1905; Rorabaugh, 1964; Berkaloff, 1967; Bagarić, 1978; Kovács, 2003; Kovács et al., 2005). These methods are based on physical principles governing the emptying of simple reservoirs, and thus assume that slow hydrograph recession purely reflects the drainage of low-permeability matrix blocks.

Other studies attempt to describe the entire recession process (including both fast and slow recessions) by fitting a series of exponential curves to different hydrograph segments (Forkasiewicz and Paloc, 1967; Atkinson, 1977; Milanovic, 1981; White, 1988; Sauter, 1992; Padilla et al., 1994; Shevenell, 1996; Baedke and Kroethe, 2001). Alternatively, they assume an exponential baseflow recession, and characterize steep recession segments by a different function (Mangin, 1975), or attempt to describe the entire recession process by one mathematical formula (Drogue, 1972).

The hydrograph decomposition technique based on exponential curve fitting generally includes three exponential components. These have been interpreted as discharge components from three individual reservoirs, representing the conduit network, an intermediate system of karstified fractures and the low-permeability matrix (Forkasiewicz and Paloc, 1967; White, 1988; Shevenell, 1996; Baedke and Kroethe, 2001). Although the numerical studies of Király and Morel (1976b) and Eisenlohr et al. (1997) demonstrated that different exponential hydrograph segments do not necessarily correspond to aquifer volumes with different hydraulic conductivities, they did not provide an adequate explanation of the several exponential segments identified on spring hydrographs.

The aim of this study is to investigate the hydraulic behavior of karst systems during recession stages in order to provide a quantitative characterization of the entire recession process. We also aim to provide a critical review on decomposition techniques.

Precedents

Hydraulic processes taking place in a karst aquifer manifest in the temporal variations in spring discharge. The plots of spring discharge versus time are referred to as spring hydrographs. Hydrographs consist of a succession of individual peaks, each of which represents the global response of the aquifer given to a precipitation event (Fig. 1). Hydrograph peaks consist of a rising and a falling limb. The rising limb comprises of a concave segment and a convex segment separated by an inflexion point. This inflexion point represents the maximum infiltration state (Király, 1998b). The falling limb comprises a steep and a slightly sloped segment. The former is called flood recession, while the latter is referred to as baseflow recession, which is the most stable section of any hydrograph. The flood recession limb is also divided into a convex segment and a concave segment by a second inflexion point, which represents the end of an infiltration event. Baseflow recession is the most representative feature of an aquifer's global response because it is the less influenced by the temporal and spatial variations of infiltration.

The first mathematical characterization of the baseflow recession was provided by Maillet (1905). This interpretation was based on the drainage of a simple reservoir and presumes that spring discharge is a function of the volume

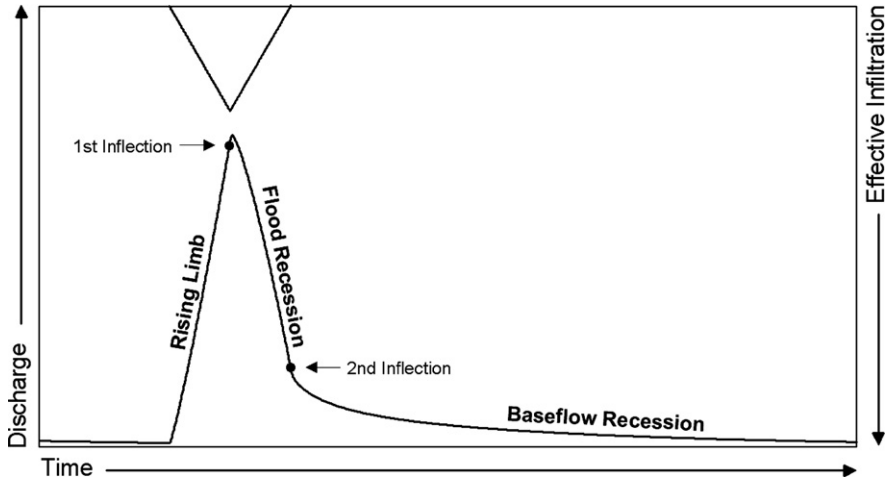

Figure 1 A schematic model of spring hydrographs. The first inflexion point corresponds to the maximum infiltration state. The second inflexion point represents the end of the infiltration event. (Modified from Kovács et al., 2005).

of water held in storage. This behavior is described by an exponential equation as follows:

$$Q_{(t)} = Q_0 e^{-\alpha t} \quad (1)$$

where Q_t is the discharge [L^3T^{-1}] at time t, and Q_0 is the initial discharge [L^3T^{-1}], α is the recession coefficient [T^{-1}] usually expressed in days. Plotted on a semi-logarithmic graph, this function is represented as a straight line with the slope $-\alpha$. This equation is usually adequate for describing baseflow recession of karst systems, and is believed to reflect the drainage of individual matrix blocks.

Rorabaugh (1964) and Berkaloff (1967) provided a quantitative link between the recession coefficient and aquifer characteristics. According to the one-dimensional analytical solution of these authors, the recession coefficient can be expressed as follows:

$$\alpha_b = \frac{\pi^2 T}{4SL^2} \quad (2)$$

where L [L] is the length of the one-dimensional domain, T [L^2T^{-1}] is hydraulic transmissivity and S [—] is storativity.

Kovács (2003) and Kovács et al. (2005) provided a two-dimensional analytical solution to the problem, and suggested that the baseflow recession coefficient may be expressed as follows:

$$\alpha_b = \frac{2\pi^2 T}{SL^2} \quad (3)$$

where L^2 is the 2D block area.

The above authors also investigated the applicability of Eq. (3) for deriving hydraulic parameters from karst systems of various configurations. This will be discussed in the following chapters.

Hydrograph decomposition

Decreasing limb of hydrograph peaks can usually be decomposed into several exponential segments. Forkasiewicz and Paloc (1967) assumed that different hydrograph segments represent different parallel reservoirs, all contributing to spring discharge (Fig. 2). They argued that such behavior reflects the existence of three reservoirs, representing the conduit network, an intermediate system of well integrated karstified fissures, and a low-permeability network of pores and narrow fissures. According to this model spring discharge can be described by the following formula:

$$Q_{(t)} = Q_1 e^{-\alpha_1 t} + Q_2 e^{-\alpha_2 t} + Q_3 e^{-\alpha_3 t} \quad (4)$$

Despite the simplicity of this interpretation, the analysis of spring hydrographs simulated by numerical models performed by Király and Morel (1976b) and later by Eisenlohr et al. (1997) showed that different exponential hydrograph segments do not necessarily correspond to aquifer volumes with different hydraulic conductivities. Three exponential reservoirs can be fitted on the hydrograph of a system consisting of only two classes of hydraulic conductivities. According to these authors, the intermediate exponential could simply be the result of transient phenomena in the vicinity of the high conductivity channels.

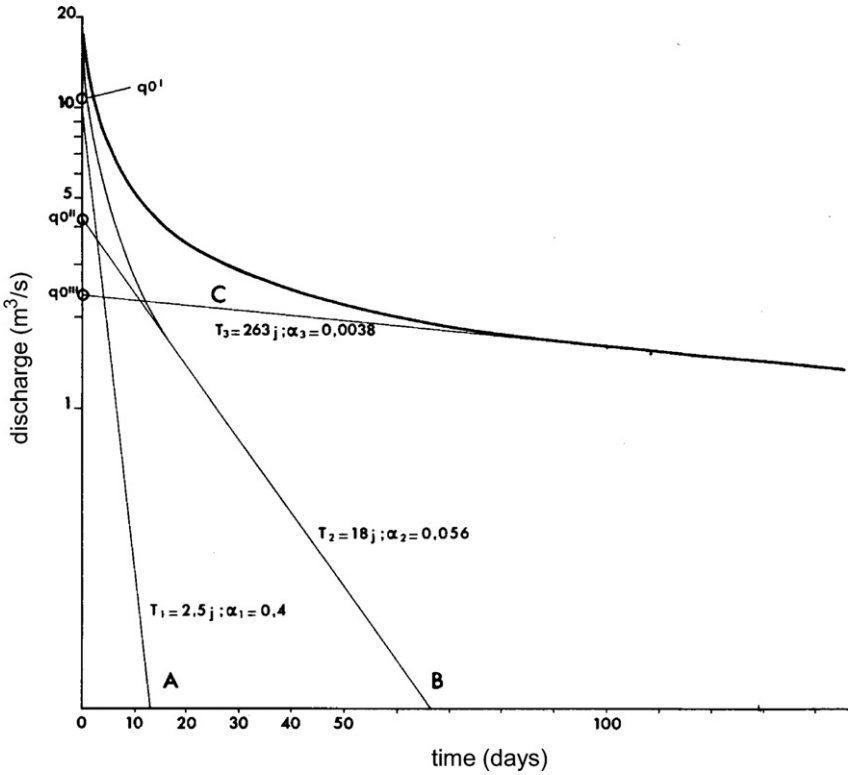

Figure 2 Decomposition of recession curves according to Forkasiewicz and Paloc (1967). ''A'' is flood recession, ''B'' is intermediate recession and ''C'' is baseflow recession. Recession components correspond to aquifer volumes with different hydraulic conductivities according to Forkasiewicz and Paloc (1967).

According to the analytical solution of Kovács (2003) and Kovács et al. (2005) for diffusive flux from a two-dimensional square block of size L encircled by uniform head boundary conditions:

$$Q_{(t)} = H_0 \frac{128}{\pi^2} T \sum_{n=0}^{\infty} e^{-(2n+1)^2 \pi^2 \frac{Tt}{SL^2}} \sum_{n=0}^{\infty} \frac{e^{-(2n+1)^2 \pi^2 \frac{Tt}{SL^2}}}{(2n+1)^2} \quad (5)$$

where initial conditions comprise uniform hydraulic heads over the block surface. Assuming that

$$a = \frac{\pi^2 Tt}{SL^2} \quad (6)$$

it follows from Eq. (5) that

$$Q_{(t)} = H_0 \frac{128}{\pi^2} T \left(e^{-2a} + \frac{10}{9} e^{-10a} + \frac{1}{9} e^{-18a} + \frac{26}{25} e^{-26a} + \frac{34}{225} e^{-34a} + \frac{1}{25} e^{-50a} + \ldots \right) \quad (7)$$

The comparison between the above analytical expression and numerical simulations shows that a sum of six series members ($n = 2$ in Eq. (5)) provides a good approximation of homogeneous block discharge (Fig. 3).

According to Eq. (7), the diffusive discharge of a single homogeneous block can be expressed as a superposition of an infinite number of exponential components. However, higher order components manifest themselves only at early times of the recession process and became negligible over a longer period of time. This explains why they cannot usually be identified on spring hydrographs based on hourly discharge data. Also, the diminution of higher order series members over time is responsible for the imaginary exponential behavior of baseflow discharge. In reality, spring discharge never exhibits perfect exponential behavior; this phenomenon is clearly experienced when numerically simulating spring hydrographs. The recession coefficient calculated for each timestep never stabilizes perfectly, but monotonously decreases with time.

The discharge hydrograph of a homogeneous square block can be decomposed into an infinite number of exponential components of which only the first six components are listed in Eq. (7). However, the weight of the different components and their temporal diminution is strongly varying. This is best seen when plotting all the exponential components together. Fig. 3 clearly indicates that components 1, 2 and 4 of the series are significant, while the remaining components 3, 5 and 6 have very little contribution to total discharge. As a matter of fact, only three exponential components contribute significantly to the total discharge of a square shaped homogeneous block. This explains why spring hydrographs are usually decomposed into three components.

However, according to this observation different hydrograph components do not represent different classes of rock permeability. Hydrographs of simple homogeneous blocks can equally be decomposed into three or more exponential segments. For a symmetric block shape however, the sum of only three exponential components provides an adequate approximation of total spring discharge (Fig. 3). The result-

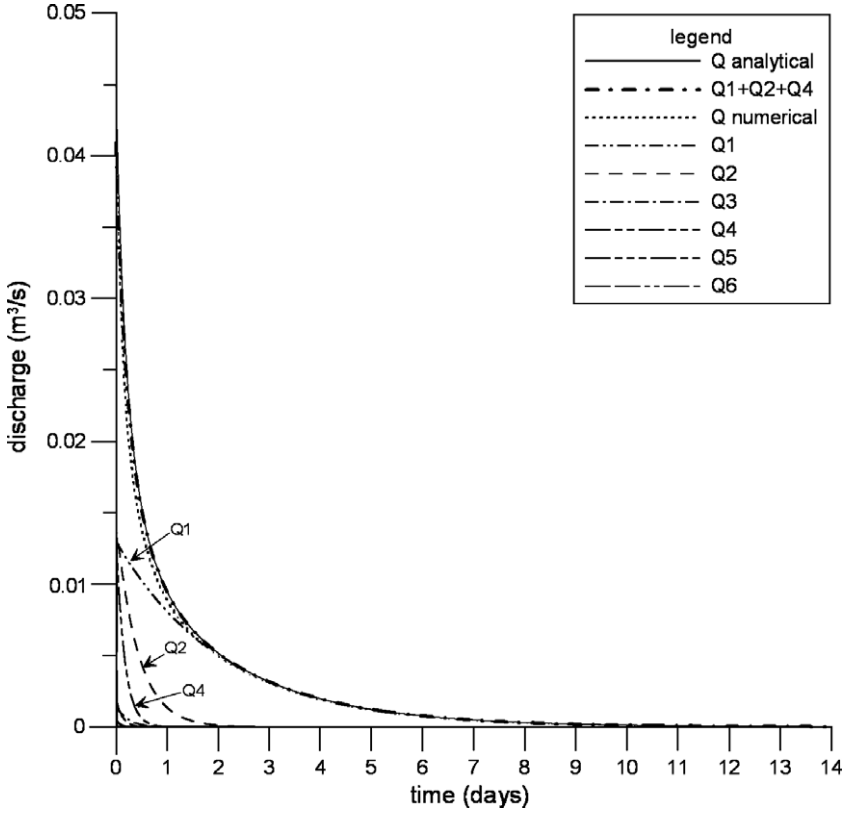

Figure 3 Analytical decomposition of discharge from a homogeneous square block. The sum of three exponential components (Q_1, Q_2, Q_4) provides a satisfactory approximation of the recession curve ($T = 10^{-5}$ m^2 s^{-1}, $S = 10^{-4}$, $L = 600$ m, $H_0 = 100$ m).

ing composite formula satisfies the hydrograph decomposition approach of Forkasiewicz and Paloc (1967):

$$Q_{(t)} \approx \frac{128}{\pi^2} H_0 T e^{-2\frac{\pi^2 Tt}{SL^2}} + \frac{1280}{9\pi^2} H_0 T e^{-10\frac{\pi^2 Tt}{SL^2}} + \frac{3328}{25\pi^2} H_0 T e^{-26\frac{\pi^2 Tt}{SL^2}} \quad (8)$$

According to this simplification, the three hydrograph recession coefficients generally identified on spring hydrographs can be expressed as follows:

$$\alpha_1 = 2\frac{\pi^2 T}{SL^2}, \quad \alpha_2 = 10\frac{\pi^2 T}{SL^2}, \quad \alpha_3 = 26\frac{\pi^2 T}{SL^2} \quad (9)$$

The numbering of recession coefficients in this study begins from the baseflow recession, and not from the flood recession as previously suggested by Forkasiewicz and Paloc (1967). Consequently, α_1 is baseflow recession coefficient, α_2 is intermediate recession coefficient, and α_3 is flood recession coefficient.

Recession of heterogeneous domains

The previous studies of Kovács (2003) and Kovács et al. (2005) demonstrated that the recession of strongly heterogeneous systems cannot be described using a single formula, but that it follows two significantly different physical principles depending on the overall configuration of the hydraulic and geometric parameter fields (Figs. 4 and 5).

The baseflow recession of mature karst systems is controlled by the recession of individual matrix blocks. This flow condition was referred to as matrix restrained flow regime (MRFR). The baseflow recession coefficient of mature karst systems can thus be expressed making use of Eq. (3) when assuming regular conduit networks with symmetric matrix block shapes.

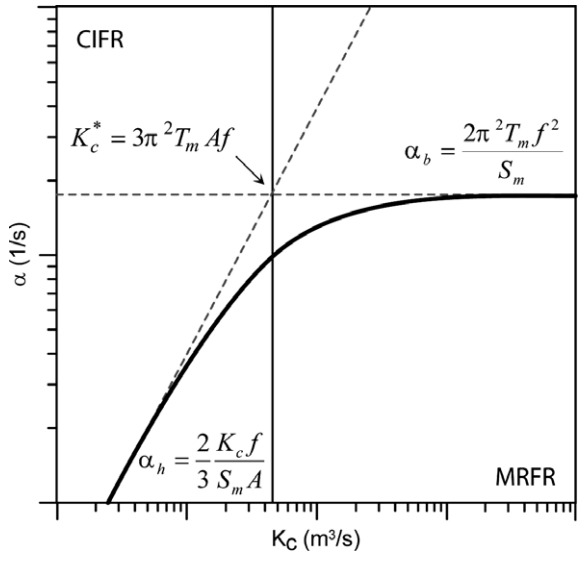

Figure 4 Dependence of the baseflow recession coefficient on conduit conductancy. K_c^* is the threshold value between MRFR and CIFR type baseflow. Modified after Kovács (2003) and Kovács et al. (2005).

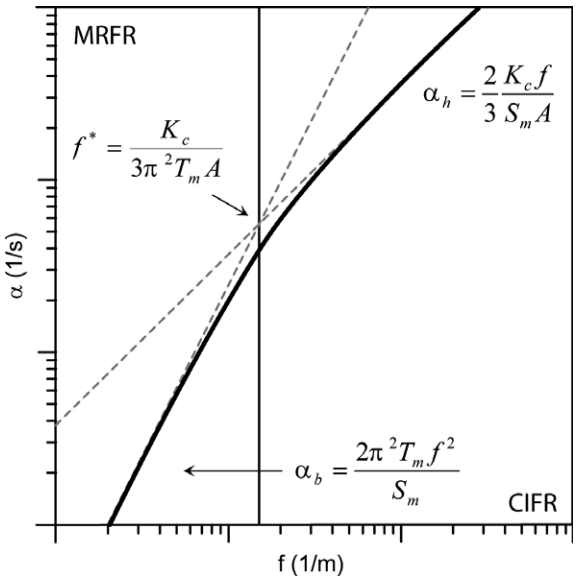

Figure 5 Dependence of the baseflow recession coefficient on conduit frequency. f^* is the threshold value between CIFR and MRFR type baseflow. Modified after Kovács (2003) and Kovács et al. (2005).

The baseflow recession of fissured systems and poorly karstified systems is influenced by the hydraulic parameters of fractures/conduits, low-permeability blocks, fracture spacing, and aquifer extent. This flow condition was defined as conduit-influenced flow regime (CIFR). The baseflow recession of fractured systems can be expressed as follows:

$$\alpha_h = \frac{2}{3}\frac{K_c f}{S_m A} \quad (10)$$

where K_c is conduit conductancy [L^3T^{-1}], f is conduit frequency [L^{-1}], S_m is matrix storativity [—] and A is the block area.

A threshold value for conduit conductancy between these two domains can be expressed as follows:

$$K_c^* \approx 3\pi^2 T_m A f \quad (11)$$

where T_m [L^2T^{-1}] is matrix transmissivity.

If the conduit conductancy of a strongly heterogeneous system exceeds the above threshold value (MRFR systems), Eq. (3) can be applied for the estimation of aquifer parameters. If conduit conductancy is inferior to the threshold value (CIFR systems), then Eq. (10) must be applied for estimating aquifer parameters.

As we intend to extend the hydrograph analytical approach to several hydrograph components of mature karst systems, only Matrix Restrained Systems (exhibiting MRFR baseflow) will be considered in this study. Our following observations are not valid for weakly karstified or fissured systems (those exhibiting CIFR baseflow).

In order to be able to extend the hydrograph analytical approach to the entire recession limb of hydrograph peaks, several model configurations have been tested by numerical models. Karstified domains containing 8 times 8 pieces of square shaped porous blocks with L = 600 m size have been simulated. A uniform initial hydraulic head of H_0 = 100 m was applied over the simulation domains. The hydraulic

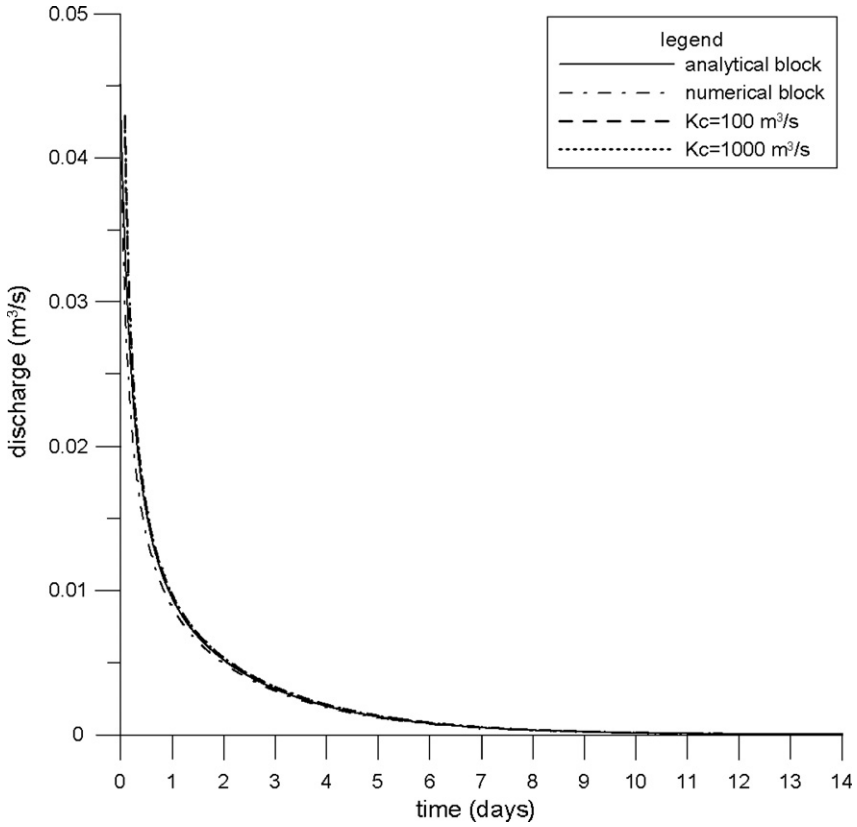

Figure 6 Comparison between analytical and numerically simulated block and spring discharges ($T = 10^{-5}$ m^2 s^{-1}, $S = 10^{-4}$, $L = 600$ m, $H_0 = 100$ m). Spring discharges have been divided by the number of matrix blocks within the simulation domain. The good correspondence between block and spring discharges indicates that the baseflow recession of Matrix Restrained systems does not depend on the hydraulic conductancy of karst conduits; it reflects the sum of total fluxes from individual matrix blocks.

conductancy of karst conduits was modified by an order of magnitude in order to demonstrate the insensitivity of spring discharge to this parameter during the entire recession process. For the sake of comparability between simulation results, the total spring discharge was divided by the number of porous blocks within the simulation domain. As demonstrated in Fig. 6, the numerically simulated spring discharges properly fit to the numerically simulated block discharge. No difference can be observed between the two spring discharge curves. Similarly, numerical and analytical block discharges show a good correspondence.

Numerical simulations confirmed that in the case of MRFR systems ($K_c > K_c^*$ in Eq. (11)) the recession process does not depend on the hydraulic conductancy of karst conduits; it reflects the sum of total fluxes from individual matrix blocks. Matrix Restrained heterogeneous systems behave similarly to a single porous block during the entire recession process, and thus hydrograph decomposition techniques developed for porous blocks can be applied to karst systems. This assumption applies when no infiltration is assumed along the conduit network.

Effect of block shape on hydrograph components

The above-discussed analytical solution (Eq. (5)) was developed for two-dimensional square blocks. As it was demonstrated by Kovács (2003) and Kovács et al. (2005), the size and the shape of a karstic water catchment do not influence the recession coefficient in the case of mature karst aquifers (Matrix Restrained Systems), nor does the hydraulic conductancy of the conduit network.

However, block shape influences the recession coefficients of MR type systems. Consequently, hydrograph components will deviate from those that were analytically expressed assuming square block shapes.

An analytical solution for diffusive flux from a two-dimensional asymmetric rectangular block encircled by uniform head boundary conditions can be expressed as follows:

$$Q_{(t)} = \frac{64TH_0}{\pi^2}\left\{\beta\sum_{n=0}^{\infty} e^{-a\beta^2(2n+1)^2}\sum_{n=0}^{\infty}\frac{e^{-a(2n+1)^2}}{(2n+1)^2} + \frac{1}{\beta}\sum_{n=0}^{\infty} e^{-a(2n+1)^2}\sum_{n=0}^{\infty}\frac{e^{-a\beta^2(2n+1)^2}}{(2n+1)^2}\right\} \quad (12)$$

where initial conditions comprise uniform hydraulic head distribution over the block surface, and

$$a = \frac{\pi^2 Tt}{SL_x^2} \quad \text{and} \quad \beta = \frac{L_x}{L_y} \quad (13)$$

L_x and L_y are block sizes in the x and y directions. It follows from Eq. (12) that

$$Q_{(t)} = \frac{64}{\pi^2} H_0 T \left\{ \begin{array}{l} \left(\beta + \frac{1}{\beta}\right) e^{-a(1+\beta^2)} + \left(\beta + \frac{1}{9\beta}\right) e^{-a(1+9\beta^2)} + \left(\frac{\beta}{9} + \frac{1}{\beta}\right) e^{-a(9+\beta^2)} + \left(\frac{\beta}{9} + \frac{1}{9\beta}\right) e^{-9a(1+\beta^2)} \\ + \left(\frac{\beta}{25} + \frac{1}{25\beta}\right) e^{-25a(1+\beta^2)} + \left(\frac{\beta}{9} + \frac{1}{25\beta}\right) e^{-a(9+25\beta^2)} + \left(\frac{\beta}{25} + \frac{1}{9\beta}\right) e^{-a(25+9\beta^2)} \\ + \left(\beta + \frac{1}{25\beta}\right) e^{-a(1+25\beta^2)} + \left(\frac{\beta}{25} + \frac{1}{\beta}\right) e^{-a(25+\beta^2)} + \ldots \end{array} \right\} \quad (14)$$

From which the baseflow recession coefficient of an asymmetric block can be expressed as follows:

$$\alpha_b = \frac{\pi^2 T}{S} \left(\frac{1}{L_x^2} + \frac{1}{L_y^2} \right) \quad (15)$$

The sum of nine series members provide a satisfactory approximation of the total discharge ($n = 2$ in Eq. (13)) as shown in Figs. 7 and 8.

By plotting the exponential components together (Fig. 7) it becomes evident that components 4, 5, 6 and 7 vanish at relatively early times of the recession process, and the sum of components 1, 2, 3, 8 and 9 properly describes the recession process for quasi symmetrical blocks. From the above solution it follows that for a symmetrical (square) block $Q_2 = Q_3$ and $Q_8 = Q_9$ and thus the recession process can be described by applying three components only (Fig. 7). However, with increasing asymmetry, term 2 diverges from term 3, and also term 8 diverges from term 9 (Fig. 8). This results in the appearance of further components on the hydrograph. Consequently, the presence of more than three significant exponential components may indicate the asymmetry of matrix blocks, and thus the anisotropy of a karst system.

Increasing block shape asymmetry results in higher initial discharges and faster recession process (Fig. 9). However, the recession of slightly asymmetric blocks can be adequately described by the symmetric recession formulation (Eq. (7)).

Simulation of flood events

The above investigations were focused on the recession of diffusive domains with uniform hydraulic head initial conditions. However, in reality, long periods of baseflow recession are interrupted by short intervals of intensive recharge.

An analytical solution for diffusive flux from an asymmetric rectangular block encircled by fixed head boundary con-

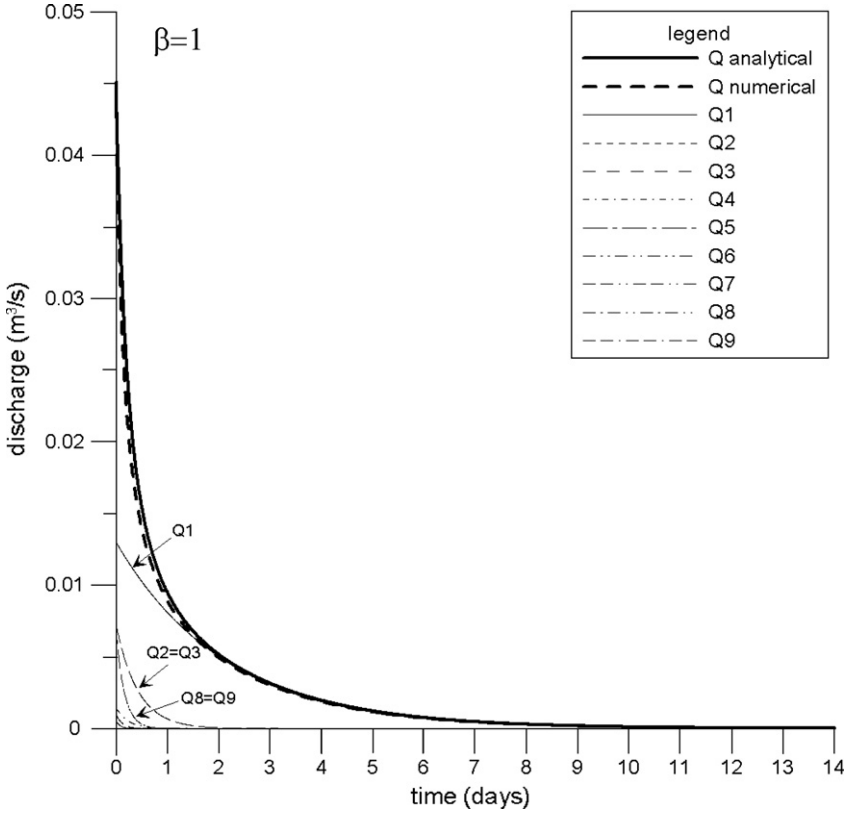

Figure 7 Asymmetric analytical hydrograph components versus numerical hydrograph ($\beta = 1$). The sum of components 1, 2, 3, 8 and 9 properly describes the recession of symmetrical blocks. For a symmetrical (square) block $Q_2 = Q_3$ and $Q_8 = Q_9$ and thus the hydrograph can be decomposed into three significant components only.

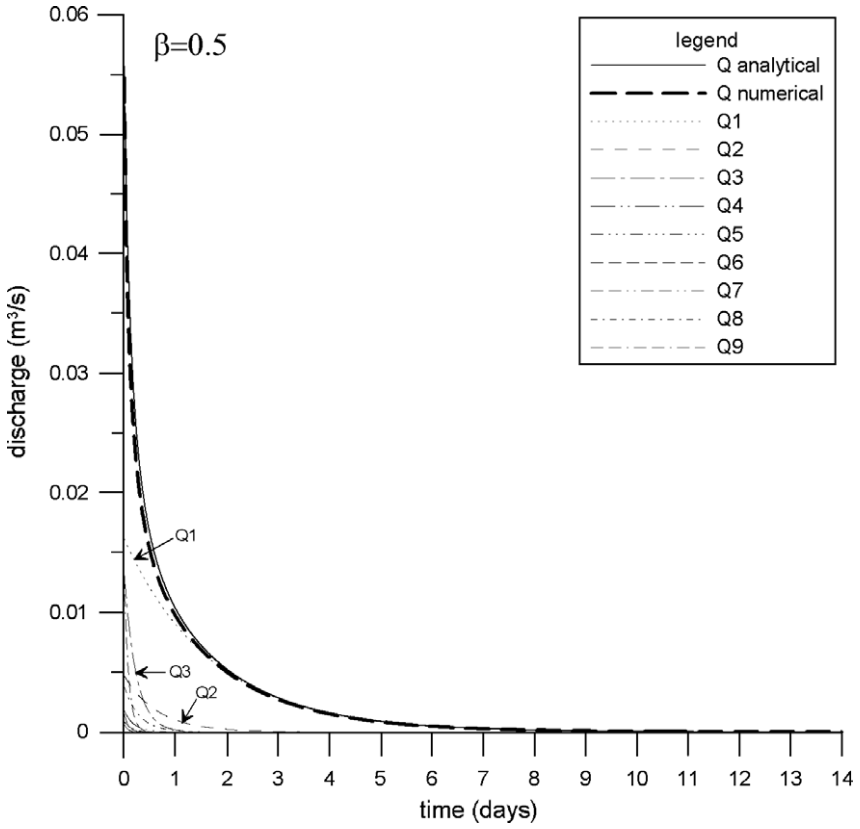

Figure 8 Asymmetric analytical hydrograph components versus numerical hydrograph ($\beta = 0.5$). With increasing asymmetry, term 2 diverges from term 3, and also term 8 diverges from term 9. This results in the appearance of further components on the hydrograph.

ditions during and following a constant recharge period over the block surface can be formulated as follows:

$$Q_{(t)} = \frac{64 i_0 L_x L_y}{\pi^4} \times \left\{ \sum_{j=0}^{\infty} \sum_{n=0}^{\infty} \frac{1-e^{-a(\beta^2(2j+1)^2+(2n+1)^2)} - H(a-a_\tau)(1-e^{-(a-a_\tau)(\beta^2(2j+1)^2+(2n+1)^2)}}{((2j+1)^2+1/\beta^2(2n+1)^2)(2n+1)^2} + \frac{1-e^{-a((2j+1)^2+\beta^2(2n+1)^2)} - H(a-a_\tau)(1-e^{-(a-a_\tau)((2j+1)^2+\beta^2(2n+1)^2)})}{((2j+1)^2+\beta^2(2n+1)^2)(2n+1)^2} \right\} \quad (16)$$

Where τ is the time corresponding to the end of the constant recharge, i_0 is the recharge rate (LT^{-1}) and $H(a-a_\tau)$ is the Heaviside function that takes the value $H = 0$ for $a \leqslant a_\tau$ and $H = a\text{-}a_\tau$ for $a > a_\tau$. From Eq. (16) if follows that the rising limb discharge is:

$$Q_{(t)} = \frac{64 i_0 L_x L_y}{\pi^4} \times \left\{ \begin{array}{l} \frac{67081}{50625} - e^{-a(1+\beta^2)} - \frac{1}{9}e^{-a(1+9\beta^2)} - \frac{1}{9}e^{-a(9+\beta^2)} - \frac{1}{81}e^{-9a(1+\beta^2)} \\ -\frac{1}{625}e^{-25a(1+\beta^2)} - \frac{1}{225}e^{-a(9+25\beta^2)} - \frac{1}{225}e^{-a(25+9\beta^2)} \\ -\frac{1}{25}e^{-a(1+25\beta^2)} - \frac{1}{25}e^{-a(25+\beta^2)} - \ldots \end{array} \right\} \quad (17)$$

and the recession limb discharge is

$$Q_{(t)} = \frac{64 i_0 L_x L_y}{\pi^4} \left\{ \begin{array}{l} \left(-e^{-a(1+\beta^2)} - \frac{1}{9}e^{-a(1+9\beta^2)} - \frac{1}{9}e^{-a(9+\beta^2)} - \frac{1}{81}e^{-9a(1+\beta^2)} \right. \\ -\frac{1}{625}e^{-25a(1+\beta^2)} - \frac{1}{225}e^{-a(9+25\beta^2)} - \frac{1}{225}e^{-a(25+9\beta^2)} \\ \left. -\frac{1}{25}e^{-a(1+25\beta^2)} - \frac{1}{25}e^{-a(25+\beta^2)} - \ldots \right) \\ + \left(e^{-(a-a_\tau)(1+\beta^2)} + \frac{1}{9}e^{-(a-a_\tau)(1+9\beta^2)} + \frac{1}{9}e^{-(a-a_\tau)(9+\beta^2)} + \frac{1}{81}e^{-9(a-a_\tau)(1+\beta^2)} \right. \\ + \frac{1}{625}e^{-25(a-a_\tau)(1+\beta^2)} + \frac{1}{225}e^{-(a-a_\tau)(9+25\beta^2)} + \frac{1}{225}e^{-(a-a_\tau)(25+9\beta^2)} \\ \left. + \frac{1}{25}e^{-(a-a_\tau)(1+25\beta^2)} + \frac{1}{25}e^{-(a-a_\tau)(25+\beta^2)} + \ldots \right) \end{array} \right\} \quad (18)$$

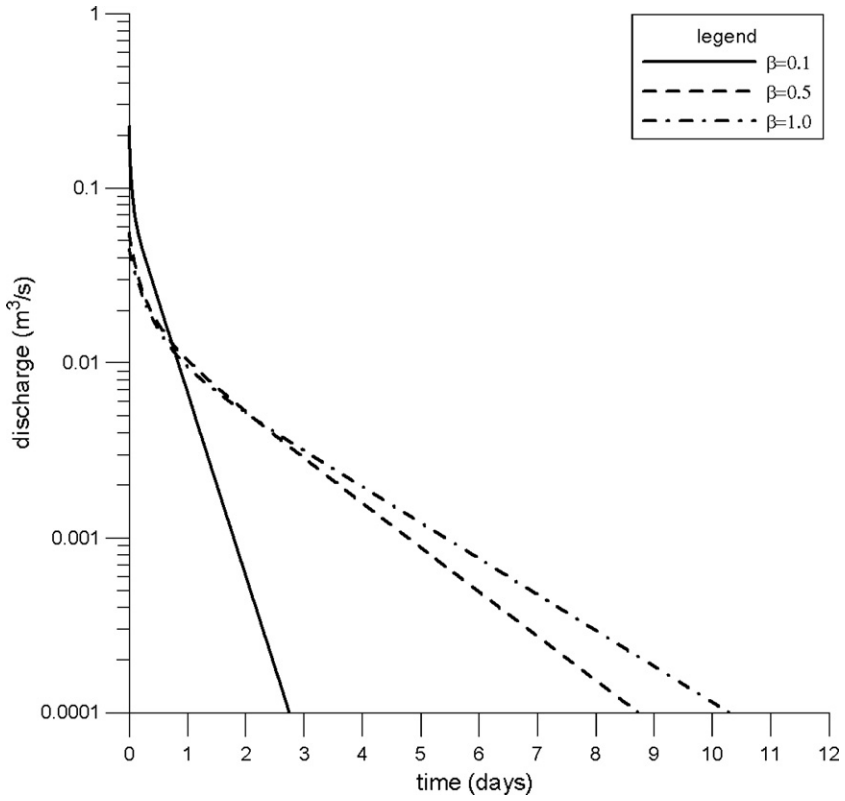

Figure 9 Analytical block discharges for different asymmetry factors. Increasing block shape asymmetry results in higher initial discharges and faster recession process.

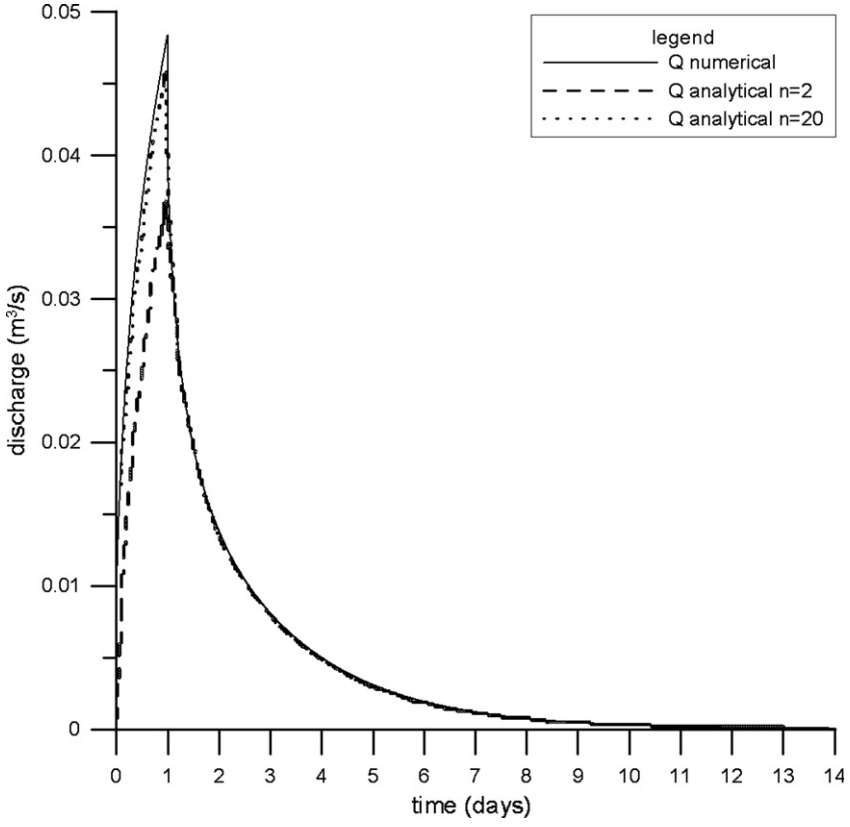

Figure 10 Comparison between analytical and numerical flood discharges. This Figure indicates the importance of high order exponential components at early times of the recharge process. The satisfactory analytical simulation of the rising limb of spring hydrographs requires the application of a large number of exponential components.

where

$$a = \frac{\pi^2 Tt}{SL_x^2} \quad \text{and} \quad a_\tau = \frac{\pi^2 T\tau}{SL_x^2} \tag{19}$$

The numerical simulation of flood discharge indicates that high order exponential components that manifest at early times of the recharge process represent a significant portion of spring discharge (Fig. 10). Consequently, the satisfactory analytical simulation of the rising limb of spring hydrographs requires the application of a large number (n = 50) of exponential components. At the same time similarly to the recession of simulation domains with uniform fixed head initial conditions, a sum of only nine series members (n = 2) provides a satisfactory approximation of the recession limb.

Effects of concentrated infiltration on spring hydrographs

The duality concept introduced by Király (1994) revealed the co-existence of diffuse and concentrated recharge during infiltration events. A part of recharge takes place in a diffusive form throughout matrix blocks, while another part originates from direct infiltration taking place at sinkholes or delivered by the high permeability epikarstic skin towards the conduit system (Mangin, 1975). According to the calculations of Jeannin and Grasso (1995), about 50% of total infiltration occurs in concentrated form.

Our investigations showed that if infiltration to a karst system takes place entirely in diffuse form, spring discharge can be calculated by simply summing individual block discharges (Figs. 11 and 12). However, if concentrated recharge is present, significantly higher peak discharges will develop. The higher proportion of concentrated recharge compared to diffuse infiltration entails higher peak discharges, but lower baseflow recession discharges. However, baseflow recession coefficient is exclusively dependent on block hydraulic characteristics and block geometry, and thus a different proportion between concentrated and diffuse discharge does not influence the value of baseflow recession coefficient.

In the case of both concentrated and diffuse recharges into an aquifer, the spring hydrograph can be reconstructed as a sum of individual block discharges and the discharge originating from the conduit network. Fig. 13 indicates the results of three different numerical simulations. In case 1 total recharge was equally distributed over matrix blocks and the conduit system. In case 2 only concentrated recharge was applied, and diffuse recharge was skipped. In case 3 only diffuse recharge was applied, and no concentrated recharge took place into the conduit system. Our numerical investigations indicate that the total discharge

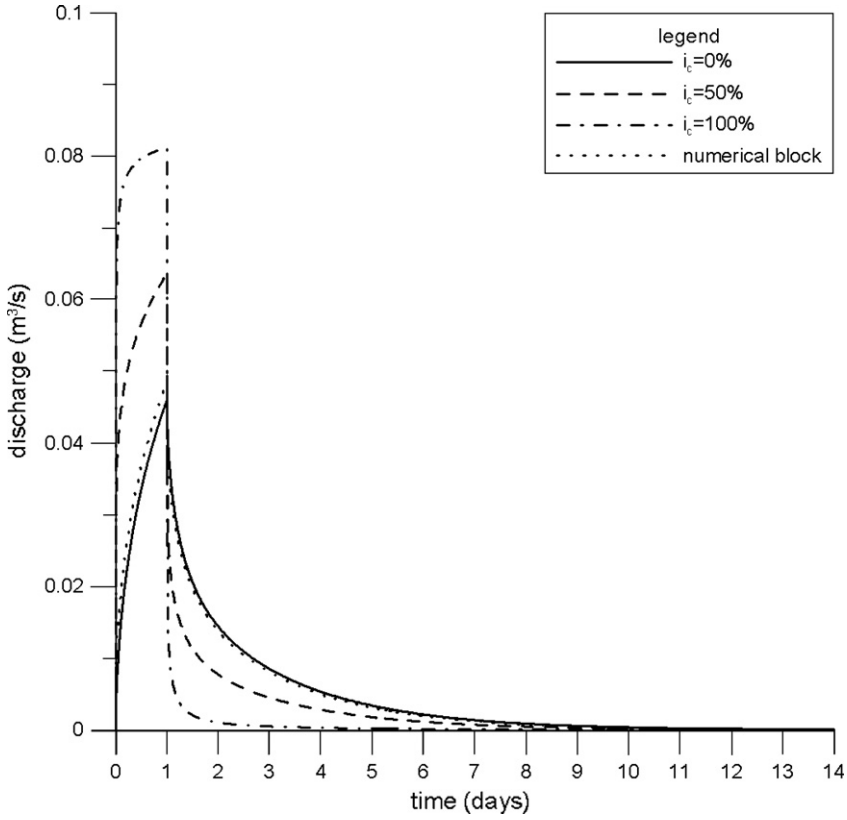

Figure 11 Numerical hydrographs showing the effect of different proportions between concentrated and diffuse infiltration. The higher proportion of concentrated recharge compared to diffuse infiltration entails higher peak discharges, but lower baseflow discharges. However, different proportion between concentrated and diffuse discharges does not influence the baseflow recession coefficient. Constant recharge has been applied.

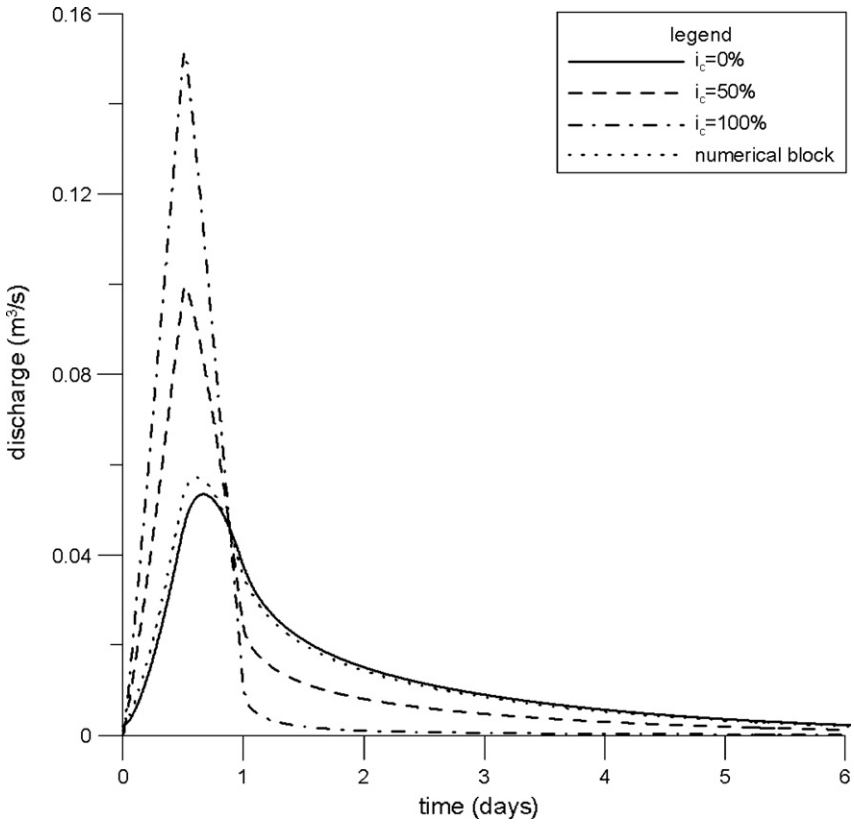

Figure 12 Numerical hydrographs showing the effect of different proportions between concentrated and diffuse infiltration. Triangular recharge function has been applied.

of case 1 (both diffuse and concentrated recharge) can be calculated by simply summing the discharge from case 2 and case 3.

The hydrograph analytical methods presented in this study are based on two-dimensional geometries. This implies semi-horizontal flow directions, and the lack of phreatic karst conduits. These assumptions are valid for most shallow karst systems. In such systems, conduit storage is generally negligible compared to the storage in matrix blocks. Among such conditions, conduit flow only has influence on the spring hydrograph until the end of the recharge event. During this period conduit discharge can be approximated by the concentrated recharge function applied and spring discharge can be evaluated as a superposition of concentrated recharge on the sum of individual block discharges. The end of an infiltration event manifests as an inflection point on hydrograph flood recession limbs (Király, 1998b). Consequently, following the inflexion of the flood recession curve, spring hydrographs can be decomposed according to the analytical solutions developed for homogeneous blocks (Eqs. (7) and (14)).

In order to prove the applicability of the above-introduced hydrograph decomposition methods, a numerically simulated spring hydrograph with known geometry, hydraulic parameters and infiltration rates has been manually decomposed using a visual curve fitting method (Fig. 14). The manually obtained recession coefficients were then compared with the analytical values (Table 1).

The comparison between manually obtained and analytically calculated results indicates a good correspondence. A negligible difference between these figures may result from numerical errors and also from the imperfect curve fitting on the baseflow recession segment. This latter issue is especially critical, since baseflow recession never manifests a perfectly exponential behavior. As lower order exponential components are successively subtracted from the discharge curve, any error in curve fitting would modify the residual discharges and thus the value of higher order recession coefficients.

Our numerical simulations suggest that the concave recession segment of any arbitrary spring hydrograph can be decomposed according to Eq. (9) when assuming symmetric block shapes. The deviation of the proportion between the recession coefficients of different hydrograph segments from those expressed in Eq. (9) may indicate block asymmetry. While aquifer parameters can be simply estimated from baseflow recession coefficient (Eqs. (3) and (15)), hypotheses on block shape can be verified, and block geometry can be estimated by applying Eq. (14). However, significant discrepancies in the proportion between the recession coefficients of different hydrograph segments may indicate not only block asymmetry but the variations of block shape or block size over the catchment area.

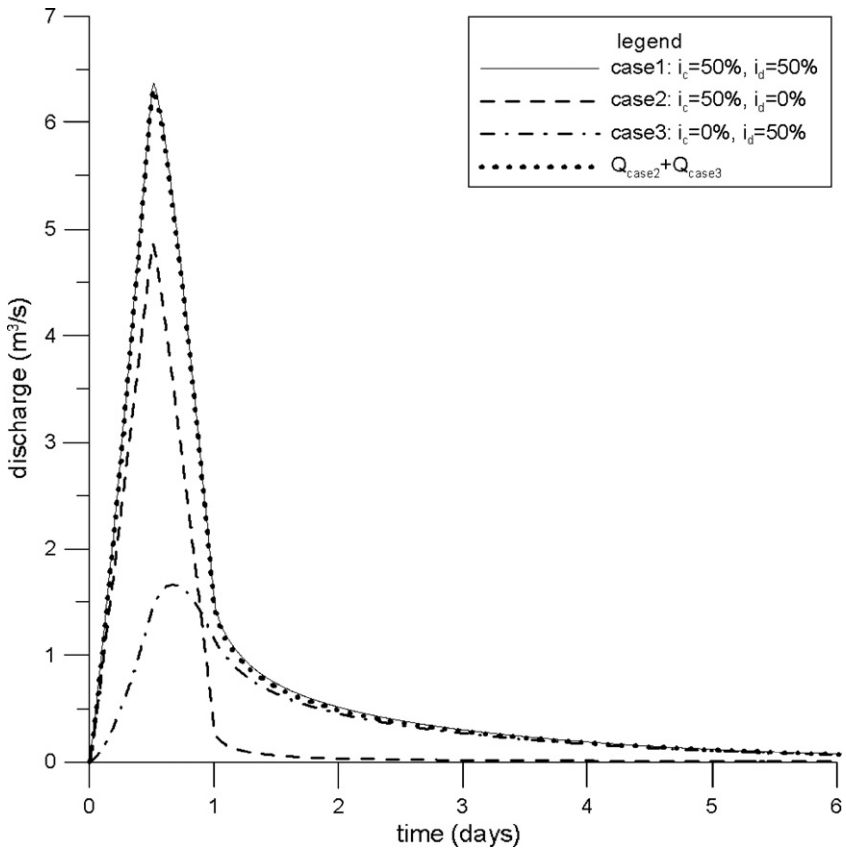

Figure 13 Numerically simulated spring discharges originating from dual, concentrated and diffuse infiltrations. Discharge originating from dual infiltration can be expressed by summing discharges originating from concentrated and diffuse recharges. In case 1 total recharge was equally distributed over matrix blocks and the conduit system. In case 2 only concentrated recharge was applied. In case 3 only diffuse recharge was applied.

Furthermore, the recession of multilevel karst systems can be a strongly nonlinear phenomenon that manifests in an erratic behavior of spring hydrographs.

Conclusions

Two-dimensional analytical solutions for diffusive flux from symmetric and asymmetric rectangular blocks have been provided. These solutions serve to analytically simulate spring hydrographs of shallow karst systems for constant recharge conditions. The same analytical solutions revealed the complex nature of diffusive discharge and suggest that hydrographs of individual homogeneous blocks can be decomposed into three or more exponential components. Consequently, different exponential components do not correspond to aquifer volumes with different hydraulic conductivities.

A systematic analysis of numerically simulated spring discharges made the extension of the analytical formulae to entire karst systems possible. When no infiltration is present, the entire recession process is controlled by the recession of individual blocks. Consequently, the hydraulic properties of a karst conduit system has no influence on spring discharge, and spring hydrographs can be simulated by summing individual block discharges.

In the case of both concentrated and diffuse recharges into an aquifer, the spring hydrograph can be reconstructed as a sum of individual block discharges and the discharge originating from the conduit network.

In the case of temporarily varying recharge, the end of the influence of conduit flow on a hydrograph manifests as an inflection point on the recession limb. Beyond this point, a hydrograph can be decomposed in a similar manner to that of an individual homogeneous block.

The hydrograph decomposition technique presented in this paper provides an insight into the hydraulic behavior of karst hydrogeological systems. Furthermore, the presented method enables the estimation of hydraulic parameters and conduit network geometry of karst aquifers. The deviation of field measurements from analytical hydrographs introduced in this study might indicate variations of block shape and size, or the presence of multi-level conduit networks.

Acknowledgement

This work was supported, in part, by the Hungarian Scholarship Board under the Eötvös Scholarship Program. The

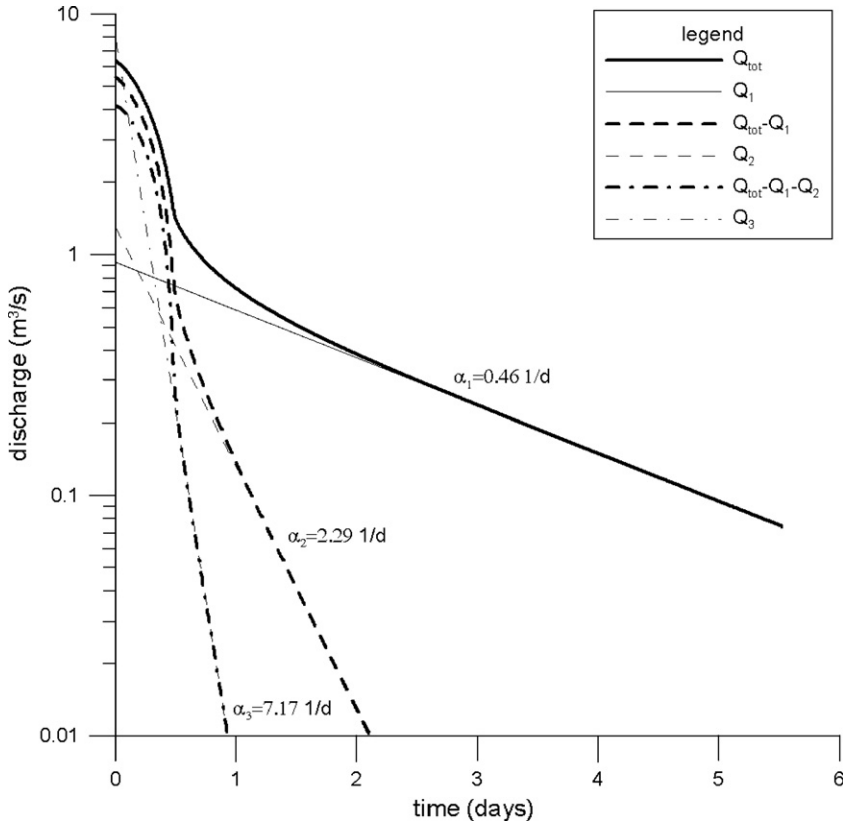

Figure 14 Manual decomposition of a numerically simulated spring hydrograph. Domain size: 4800×4800 m, $L = 600$ m, $T_m = 10^{-5}$ m^2/s, $S_m = 10^{-4}$, $K_c = 100$ m^3/s, $S_c = 2.14 \times 10^{-7}$. A triangular recharge function with $i_{max} = 20$ mm/d over 24 h has been applied. Concentrated infiltration was 50% of total recharge.

Table 1 Comparison between numerical and analytical recession coefficients

	Numerical	Analytical
α_1	5.30E−06	5.48E−06
α_2	2.65E−05	2.74E−05
α_3	8.30E−05	7.13E−05

Numerical values result from manual decomposition and curve fitting of a numerically simulated hydrograph.

authors would like to thank L. Bell for a review of the draft of this work.

References

Atkinson, T.C., 1977. Diffuse flow and conduit flow in limestone terrain in the Mendip Hills, Somerset (Great Britain). Journal of Hydrology 35, 93—103.

Baedke, S.J., Kroethe, N.C., 2001. Derivation of effective hydraulic parameters of a karst aquifer from discharge hydrograph analysis. Water Resources Research 37, 13—19.

Bagarić, I., 1978. Determination of storage and transportation characteristics of karst aquifers. In: Milanović, P.T. (Ed.), Karst hydrogeology. Water Resources Publications, Littleton, CO, USA, 434 p.

Berkaloff, E., 1967. Limite de validité des formules courantes de tarissement de débit. Chronique d'Hydrogéologie 10, 31—41.

Drogue, C., 1972. Analyse statistique des hydrogrammes de décrues des sources karstiques. Journal of Hydrology 15, 49—68.

Eisenlohr, L., Király, L., Bouzelboudjen, M., Rossier, I., 1997. A numerical simulation as a tool for checking the interpretation of karst springs hydrographs. Journal of Hydrology 193, 306—315.

Forkasiewicz, J., Paloc, H., 1967. Le régime de tarissement de la Foux-de-la-Vis. Etude préliminaire. Chronique d'Hydrogéologie, BRGM 3 (10), 61—73.

Jeannin, P.-Y., Grasso, A.D., 1995. Estimation des infiltrations efficaces journalières sur le bassin karstique de la Milandrine (Ajoie, JU, Suisse). Bulletin d'Hydrogéologie de l'Université de Neuchâtel 14, 83—89.

Király, L., 1994. Groundwater flow in fractures rocks: models and realityProceedings of the 14th Mintrop Seminar über Interpretationsstrategien in Exploration und Produktion, vol. 159. Ruhr Universität Bochum, pp. 1—21.

Király, L., 1998a. Modeling karst aquifers by the combined discrete channel and continuum approach. Bulletin d'Hydrogéologie, Neuchâtel 16, 77—98.

Király, L., 1998b. Introduction à l'hydrogéologie des roches fissurées et karstiques. Bases théoriques à l'intention des hydrogéologues. Manuscrit, Université de Neuchâtel.

Király, L., 2002. Karstification and Groundwater Flow. In: Proceedings of the Conference on Evolution of Karst: From Prekarst to Cessation. Postojna-Ljubljana, pp. 155—190.

Király, L., Morel, G., 1976a. Etude de régularisation de l'Areuse par modèle mathématique. Bulletin d'Hydrogéologie, Neuchâtel 1, 19—36.

Király, L., Morel, G., 1976b. Remarques sur l'hydrogramme des sources karstiques simule par modèles mathématiques. Bulletin d'Hydrogéologie, Neuchâtel 1, 37—60.

Kovács, A., 2003. Geometry and hydraulic parameters of karst aquifers: a hydrodynamic modeling approach. Doctoral Thesis, University of Neuchâtel, Switzerland, 131 p.

Kovács, A., Perrochet, P., Király, L., Jeannin, P.-Y., 2005. A quantitative method for the characterization of karst aquifers based on spring hydrograph analysis. Journal of Hydrology 303, 152—164.

Maillet, E., 1905. Essais d'hydraulique souterraine et fluviale. Hermann, Paris.

Mangin, A., 1975. Contribution a l'étude hydrodynamique des aquifères karstiques. Thèse, Institut des Sciences de la Terre de l'Université de Dijon.

Milanovic, P.T., 1981. Karst hydrogeology. Water Resources Publications, Littleton, CO, 434p.

Padilla, A., Pulido-Bosch, A., Mangin, A., 1994. Relative importance of baseflow and quickflow from hydrographs of karst springs. Ground Water 32 (2), 267—277.

Rorabaugh, M.I., 1964. Changes in bank storage. Publication No. 63, IASH, Gentbrugge, 432—441.

Sauter, M., 1992. Quantification and forecasting of regional groundwater flow and transport in a karst aquifer (gallusquelle, malm, SW. Germany). Ph.D. thesis, University of Tübingen.

Shevenell, L., 1996. Analysis of well hydrographs in a karst aquifer: estimates of specific yields and continuum transmissivities. Journal of Hydrology 174, 331—355.

White, W.B., 1988. Geomorphology and hydrology of karst terrains. Oxford University Press, New York, 464p.